Influence of strain on the magnetocrystalline anisotropy in epitaxial Cr/Co/Pd(111) films

S. Boukari, E. Beaurepaire, H. Bulou, B. Carrière, J. P. Deville, and F. Scheurer
Institut de Physique et Chimie des Matériaux de Strasbourg, UMR 7504, CNRS–Université Louis Pasteur, 23 rue du Loess, 67037 Strasbourg, France

M. De Santis and R. Baudoing-Savois
Laboratoire de Cristallographie, CNRS (UPR 5031) associé à l'Université J. Fourier et à l'Institut National Polytechnique de Grenoble, 25 av. des Martyrs, 38042 Grenoble, France

(Received 6 February 2001; published 24 September 2001)

We studied the correlations between the structure (in particular strain) and magnetic anisotropy in thin Co/Pd(111) films uncovered and covered with Cr. Measurements were done by grazing incidence x-ray diffraction and magneto-optical Kerr effect. To properly describe these correlations, one has to consider a surface magnetoelastic coefficient. We demonstrate that Cr capping leads to an enhanced anisotropy strength due to strain effects, and an extended perpendicular anisotropy thickness range due to an interface contribution.

DOI: 10.1103/PhysRevB.64.144431 PACS number(s): 75.70.Ak, 75.80.+q, 75.30.Gw

Magnetic multilayers and ultrathin films often present enhanced perpendicular anisotropy that make them suitable for application in the field of magnetic recording or storage devices.[1] Their anisotropy properties are usually described phenomenologically by the Néel pair interaction model.[2] In this picture, the tendency for the magnetization to be out-of-plane results from the competition between a surface (or interface) anisotropy (K_s), due to the broken symmetry, and the volume (K_v) plus the dipolar anisotropy (K_{dip}). The effective anisotropy is given by

$$K = K_v + K_{\mathrm{dip}} + K_s/d, \tag{1}$$

where d is the thickness of the film.[3]

However, epitaxial films usually present a strain dependence with thickness so that K_v is no longer constant but depends on the thickness d because of magnetostriction.[4–6] If this is not taken into account, as in Eq. (1), it results in an apparent contribution to K_s from the strain dependence of K_v, although the energy is located throughout the film and not only at the interfaces.[7] The surface anisotropy K_s obtained from such an analysis must therefore be viewed as an effective anisotropy.

Strain induced modification of the anisotropy could also appear upon capping a film with a protective layer (to perform *ex situ* magnetic measurements for instance), as it is known that capping can have a strong effect on the underlaying film structure.[8]

We see therefore that the connection between the macroscopic anisotropy and the structural parameters can be complex. Often one could be tempted to infer, from the dependence of anisotropy on thickness, the structural properties at the origin of this anisotropy. However such a process can easily lead to erroneous conclusions about the structure, which in the end hinder the efforts made to engineer the anisotropy.

To disentangle the origin of the different contributions to the anisotropy, we made a study of the interplay between the magnetic anisotropy and the structure in Co/Pd(111) and Cr/Co/Pd(111) films. In particular, the influence of the capping on the strain state in the Co layer is analyzed.

The magnetic characterization was performed by *in situ* and *ex situ* magneto-optical Kerr effect (MOKE). The in-plane and out-of-plane strains as well as the stacking of the Co layers were determined by *in situ* grazing x-ray diffraction (GIXD), performed at the SUV station of the French CRG-IF beamline (BM32) at the European Synchrotron Radiation Facility in Grenoble.[9] The chamber allows simultaneous *in situ* film growth and diffraction measurements. The energy of the impinging beam was 11 keV and the incident angle was kept above the critical angle for total reflection. The reciprocal lattice was described by **A***, **B***, and **C*** with **A***, **B*** in the surface plane making an angle of 60° and **C*** normal to the surface: $\|\mathbf{A}^*\| = \|\mathbf{B}^*\| = 4\pi\sqrt{2}/a_{Pd}\sqrt{3} = 2.642\ \text{Å}^{-1}$ and $\|\mathbf{C}^*\| = 2\pi/a_{Pd}\sqrt{3} = 0.9342\ \text{Å}^{-1}$. For more details on sample preparation and diffraction experiments, see Ref. 10.

The Co was deposited by molecular beam epitaxy at 370 K on a Pd(111) single crystal to obtain smoother films than those deposited at 300 K.[11] The magnetic properties of uncovered Co/Pd(111) were measured *in situ* by MOKE in the polar geometry during the growth at 370 K. The loops show full remanence between 2.0 and 4.3 monolayers (ML), indicating a perpendicular easy axis (Fig. 1). Upon covering the Co layer with Cr, the perpendicular region with full remanence is extended to 7 ML. This behavior is due to a change in the *effective* interface anisotropy, favoring a perpendicular easy axis. However, to know whether the change is located at the Co-Cr interface or in the volume of the film, one has to check if Cr deposition induces structural changes in the underlying Co film.

The in-plane lattice parameter of uncovered Co films grown on Pd(111) was measured *in situ* as a function of Co thickness by GIXD during the growth by locating the maximum of the so-called Co truncation rod (see Fig. 2). A rod denotes the intensity diffracted between Bragg points because of finite size effects. The position of a rod perpendicular to the surface is related to the in-plane lattice parameter.[10,12] Since the penetration depth of the beam is

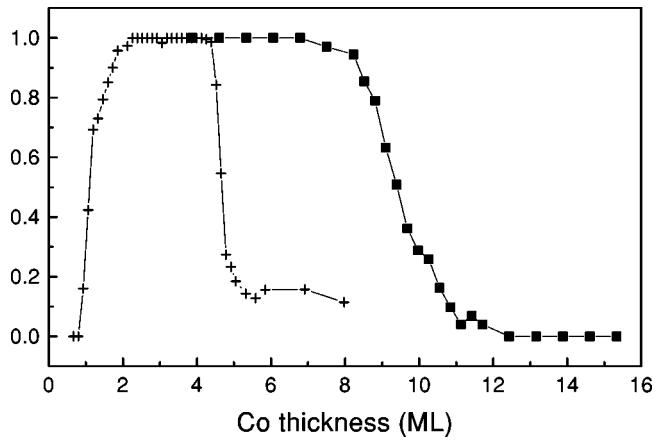

FIG. 1. Remanence divided by saturation for uncovered Co/Pd(111) films (crosses), and covered wih Cr (squares).

much larger than the film thickness, an average lattice parameter of the Co film is obtained. We tried several models to fit the relaxation with thickness d of the in-plane lattice parameter: a $1/d$ decrease,[7] a $(1/d)^{2/3}$ decrease,[13] and a model proposed by Basson and Ball.[14] In our case, these models do not give a satisfactory description of our data. The in-plane strain is rather described by the following phenomenological law when $d > d_i$

$$\varepsilon_{\parallel}(d) = \eta[\alpha + (1-\alpha) d_c/(d-d_i)], \tag{2}$$

where η=9.8% is the natural misfit between Co and Pd, and α accounts for a residual strain. Similar descriptions of strain relaxation were made in the case of Ni/Cu(100),[15] Co/W(110),[16] and Co/Cu(100).[17] The best fit is obtained with α=0.14, d_c=0.42 ML, and d_i=1.72 ML. Comparable values of residual strain (about 1.5%) were also observed on Co/Pd(111) multilayers.[18]

After Cr deposition on the Co/Pd(111) films, the in-plane Co lattice parameter is modified (see Fig. 2). There is an

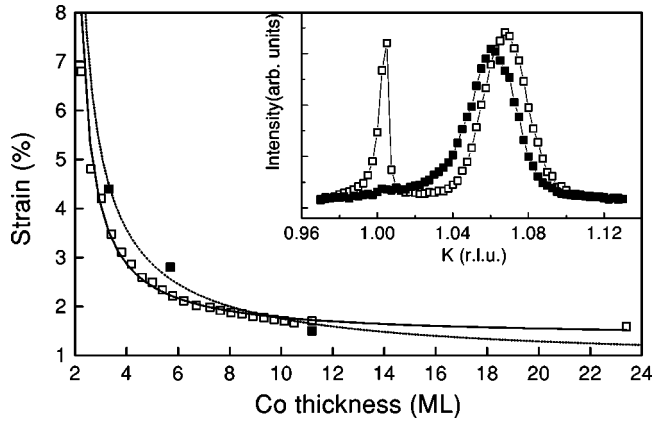

FIG. 2. In plane strain for an uncovered (open squares) Co/Pd(111) film and covered (full squares) with 14 Cr ML. The lines are fits to the data (see text). The inset shows the diffracted intensity around the Pd (K=1) and Co (K~1.6) truncation rod at H=0 and L=0.4 for a 5.7 ML Co film. Note the change in position of the Co truncation rod (right) before (open squares) and after (full squares) Cr coverage. The K scale is in reciprocal lattice units.

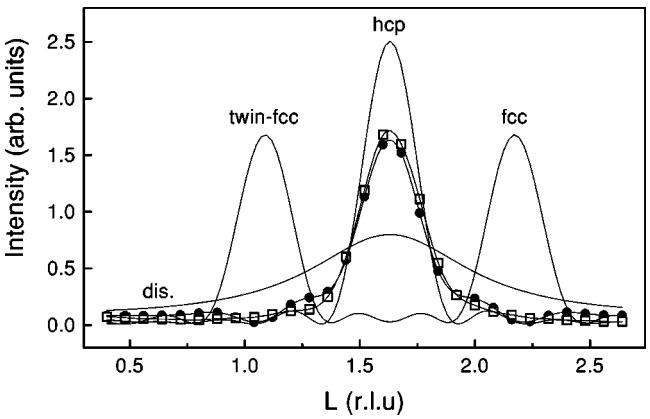

FIG. 3. X-ray intensity along the Co truncation rod for a 14 ML Cr/ 11 ML Co/Pd(111) film. The L scale is in reciprocal lattice units. Open squares represent the data points. The best fit represented by full circles was obtained with a 50% hcp and a 50% disordered stacking. Indicated is the intensity which would arise from a pure disordered, twin-fcc, hcp, or fcc film.

expansion at low Co thicknesses and strain release at higher thicknesses. To account for the Cr capping on the in-plane Co strain, we kept the same functional description for the strain as for uncovered Co/Pd(111) and added two terms. The new strain is given by

$$\varepsilon'_{\parallel}(d) = \varepsilon_{\parallel}(d) + a/d + b, \tag{3}$$

with $a = 4.6\% \cdot$ ML and $b = -0.5\%$. We emphasize that the above formula is used as a purely phenomenological description of strain modifications. Our point is not to analyze the relaxation mechanism but to obtain numerical values for the strain as a function of Co thickness.

Scanning along the Co truncation rod perpendicular to the film plane makes it possible to distinguish between the different stacking sequences of the Co planes and to determine the spacing of the planes. Using Guinier's model,[19] the data are fitted with a combination of hcp, fcc and twinned fcc, and disordered contributions (Fig. 3). No significant evolution in the stacking or in the interlayer parameter (deduced from the position of the maximum of the peaks) is noticed upon Cr deposition. On average, the covered films are slightly expanded out-of-plane by about 1.2 % with respect to the bulk value for hcp Co (2.04 Å=1 ML). According to the macroscopic elasticity laws, an expansion both in-plane and out-of-plane is unexpected but has already been observed. It has been attributed to the defects in the film.[20,21] The films are composed of about 50% hcp Co and 50% disordered Co (see Fig. 3). If the stacking sequence of an fcc structure is characterized by the letters *ABC* . . . and the one for an hcp structure by *ABAB* . . . , then by disordered Co we mean that on top of a plane *A*, there is the same probability to have a plane *B* or *C*. Regarding the magnetic anisotropy, a disordered film is equivalent to a film made half of fcc Co and half of hcp Co, so that the magnetic properties of our film will be described by a film with 25% fcc Co and 75% hcp Co.

The modification of magnetic properties upon Cr capping is therefore a complex effect. K_v is no longer constant but depends on the Co thickness through the thickness depen-

TABLE I. Tabulated material dependent parameters used to describe the anisotropy.

K_{dip} 10^6 erg/cm^3	K_{mc}^{hcp} 10^6 erg/cm^3	$B_1^{hcp}+2B_3^{hcp}$ 10^6 erg/cm^3	B_2^{hcp} 10^6 erg/cm^3	B_2^{fcc} 10^6 erg/cm^3
−12.6	4.1[a]	570[b]	−220[c]	770[d]

[a]Reference 23.
[b]Reference 24.
[c]Reference 24.
[d]Reference 25.

dence of strain. To estimate the strain contribution to the effective anisotropy K, we modeled the anisotropy starting from a structural description and including parameters found in the literature about magnetic properties of Co (see Table I). The model result was then compared to the measured anisotropy, which was obtained by fitting polar hysteresis loops with a Stoner-Wohlfarth coherent rotation model assuming a magnetization of 1420 emu/cm^3 for the Co. The loops were recorded *ex situ* on a wedge-shaped Co/Pd(111) film covered with Cr. To ensure coherent rotation of the magnetization they were acquired by polar MOKE in two different geometries: perpendicular magnetic field when the easy axis of magnetization was in-plane, and with a magnetic field at 79° from the normal for a perpendicular easy axis.[22] Typical magnetization loops for both geometries are represented in Fig. 4 with the best fit in full line (taking into account a fourth order term). However, the effective anisotropy could not be determined in the thickness range from 7 to 11 ML, for which there is evidence of noncoherent magnetization rotation.

On the plot $K\cdot d$ versus thickness, one observes a nonlinear behavior at low thicknesses which is not compatible with Eq. (1) (Fig. 5). This curvature shows the tendency for the magnetization to go back in-plane. Using Eq. (1) to extrapolate the high thickness data gives an effective interface anisotropy K_s of 1.38 erg/cm^2 and a volume anisotropy K_v of 4.4×10^6 erg/cm^3.

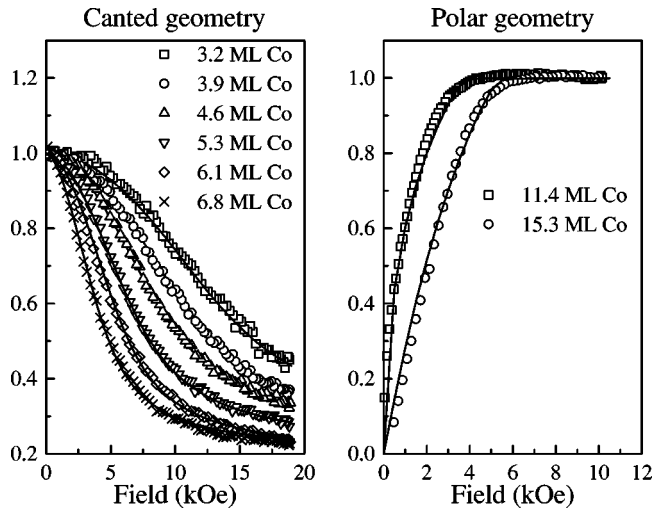

FIG. 4. Normalized magnetization curve recorded in a canted and polar geometry on a Co wedge covered with Cr. The uniaxial anisotropy was deduced from fits to the data (full lines) using a coherent rotation model including first and second order anisotropy.

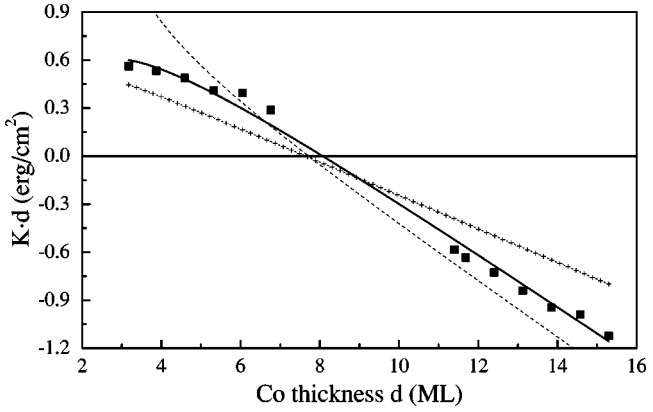

FIG. 5. Anisotropy times Co thickness versus Co thickness for a Co wedge covered with Cr. The full line is a fit to the data (full squares) using Eq. (4) and material dependent parameters given in Table I. The dashed curve results from a fit with no interface magnetoelastic coupling constant ($B_s=0$). The crossed line is obtained with $a=b=0$ in Eq. (3) to estimate the strain induced anisotropy change upon Cr capping (see text).

Note that the effective volume anisotropy is close to the one for an unstrained hcp Co thin film (see Table I), so that from the slope alone one would conclude that there is no strain in the film.

From the detailed structural description given above, we modeled the magnetic uniaxial anisotropy using the following expression:

$$K=K_{dip}+0.75[K_{mc}^{hcp}+(B_1^{hcp}+2B_3^{hcp})\varepsilon_{\parallel}'+B_2^{hcp}\cdot\varepsilon_{\perp}]+0.25\cdot B_2^{fcc}(\varepsilon_{\parallel}'-\varepsilon_{\perp})+2(\mathbf{K}_s+\mathbf{B}_s\cdot\varepsilon_{\parallel}')/d, \quad (4)$$

where everything is known except two parameters which are designed in bold in the equation: K_{dip} is the dipolar anisotropy, K_{mc}^{hcp} the hcp Co magnetocrystalline anisotropy, K_s the Néel interface anisotropy, and the B_i's (respectively B_s) are first order bulk (respectively surface) magnetoelastic coupling constants. The Co fcc magnetocrystalline anisotropy and the effect of roughness on the anisotropy were neglected. The convention is that a positive K denotes a perpendicular easy axis. Values used for the material dependent parameters are given in Table I. The two unknown parameters—the interface anisotropy K_s and the surface magnetoelastic constant B_s—are used to fit the data.

A first attempt to fit the data was done with B_s fixed to zero. The best result (dashed curve of Fig. 5) was obtained with $K_s=0.08$ erg/cm^3. Clearly the fitting is not satisfactory, especially at low thicknesses where the curvature is opposite to the measured one. At higher thicknesses however the slope is close to the one given by the data.

A second attempt was therefore needed where the two parameters K_s and B_s were free to vary during the fit. Now the data are well described (full line of Fig. 5) with $K_s=0.34$ erg/cm^3 and $B_s=-11.5$ erg/cm^2. Also the tendency for the magnetization to go back in-plane is accounted

for through the negative value of B_s. The influence of the surface magnetoelastic constant is therefore opposite to the interface anisotropy. Note that the as fitted interface anisotropy $K_s = 0.34$ erg/cm^3 is much smaller than the one deduced from the simple model [Eq. (1), leading to $K_s = 1.38$ erg/cm^3], which demonstrates how large the magnetoelastic contribution to the effective interface anisotropy can be.

To try to understand how Cr deposition changes the magnetic anisotropy, the function $K \cdot d$ is plotted with the previously evaluated K_s and B_s, taking $a = b = 0$ in Eq. (3) (crossed curve of Fig. 5) to virtually hinder the deformations in the magnetic film due to capping. The slope of the as obtained curve is smaller than the one corresponding to the data. The deformation induced by Cr increases thus the strength of the anisotropy over the whole thickness range. However, the thickness where the easy axis switches from perpendicular to parallel to the surface is nearly the same as when Cr induced deformations are included. The extension of region with full perpendicular remanence upon Cr deposition (see Fig. 1) is therefore mainly due to an increase of the interface anisotropy.

In summary, structural and magnetic investigation of uncovered Co/Pd(111) films and then covered with Cr has been performed. Through a detailed analysis of the structure of the film, we were able to show up the correlations between the structure and the anisotropy. Capping the Co film with Cr has two effects: first an increase of the interface anisotropy which leads to an extension of the region with full perpendicular remanence, and second a deformation of the underlaying Co film which increases the strength of the anisotropy. To properly describe the magnetic anisotropy, in particular towards the low thicknesses, one has to consider a surface magnetoelastic coefficient.

Beam time at ESRF (French CRG-Interface beamline) is acknowledged for the present study via the French Scientific Committee.

[1] M.T. Johnson, P.J.H. Bloemen, F.J.A. den Broeder, and J.J. de Vries, Rep. Prog. Phys. **59**, 1409 (1996).
[2] L. Néel, J. Phys. Radium **15**, 376 (1954).
[3] See, e.g., W.J.M. de Jonge, P.J.H. Bloemen, and F.J.A. den Broeder, in *Ultrathin Magnetic Structures I*, edited by B. Heinrich and J.A.C. Bland (Springer-Verlag, Berlin, 1994), p. 65; J.-P. Renard, in *Magnetism and Synchrotron Radiation*, edited by E. Beaurepaire, B. Carrière, and J.-P. Kappler (Editions de Physique, Les Ulis, 1996), p. 185.
[4] B. Schulz and K. Baberschke, Phys. Rev. B **50**, 13 467 (1994).
[5] Kin Ha and R.C. O'Handley, J. Appl. Phys. **85**, 5282 (1999).
[6] For a review of magnetoelastic effects in thin films, see D. Sander, Rep. Prog. Phys. **62**, 1 (1999).
[7] C. Chappert and P. Bruno, J. Appl. Phys. **64**, 5736 (1988).
[8] H. Magnan, D. Chandesris, B. Villette, O. Heckmann, and J. Lecante, Phys. Rev. Lett. **67**, 859 (1991); Ch. Rath, J.E. Prieto, S. Müller, R. Miranda, and K. Heinz, Phys. Rev. B **55**, 10 791 (1997).
[9] R. Baudoing-Savois, M. De Santis, M.-C. Saint-Lager, P. Dolle, O. Geaymond, P. Taunier, P. Jeantet, G. Renaud, A. Barbier, O. Robach, O. Ulrich, A. Mougin, and G. Berard, Nucl. Instrum. Methods Phys. Res. B **149**, 213 (1999); **159**, 210(E) (1999).
[10] S. Boukari, E. Beaurepaire, H. Bulou, B. Carrière, J.-P. Deville, F. Scheurer, R. Baudoing-Savois, and M. De Santis, Surf. Sci. **430**, 37 (1999).
[11] S. Boukari, Ph.D. thesis, Université Louis Pasteur, Strasbourg, 1998.
[12] I.K. Robinson, Phys. Rev. B **33**, 3830 (1986).
[13] K. Ha, M. Ciria, R.C. O'Handley, P.W. Stephens, and P. Pagula, Phys. Rev. B **60**, 13 780 (1999).
[14] J.H. Basson and C.A.B. Ball, Phys. Status Solidi A **46**, 707 (1978).
[15] J.W. Matthews and J.L. Crawford, Thin Solid Films **5**, 187 (1970).
[16] H. Fritzsche, J. Kohlhepp, and U. Gradmann, Phys. Rev. B **51**, 15 933 (1995).
[17] W. Weber, A. Bischof, R. Allenspach, C.H. Back, J. Fassbender, U. May, B. Schirmer, R.M. Jungblut, G. Güntherodt, and B. Hillebrands, Phys. Rev. B **54**, 4075 (1996).
[18] F. Hakkens, A. De Veirman, W. Coene, and F.J.A. den Broeder, J. Mater. Res. **8**, 1019 (1993).
[19] *X-ray Diffraction in Crystals, Imperfect Crystals and Amorphous Bodies*, edited by A. Guinier (Dover, New York, 1994).
[20] F.J. Lamelas, H.D. He, and R. Clarke, Phys. Rev. B **43**, 12 296 (1991).
[21] S. Ferrer, J. Alvarez, E. Lundgren, X. Torrelles, P. Fajardo, and F. Boscherini, Phys. Rev. B **56**, 9848 (1997).
[22] S.T. Purcell, M.T. Johnson, N.W.E. McGee, W.B. Zeper, and W. Howing, J. Magn. Magn. Mater. **113**, 257 (1992).
[23] R. Allenspach, J. Magn. Magn. Mater. **129**, 160 (1994).
[24] V.F. Taborov and V.F. Tarasov, Fiz. Tverd. Tela (St. Petersburg) **34**, 2959 (1992) [Sov. Phys. Solid State **34**, 1588 (1992)].
[25] H. Takahashi, S. Tsunashima, S. Iwata, and S. Uchiyama, J. Magn. Magn. Mater. **126**, 282 (1993); the value of B_2^{fcc} was deduced by extrapolating the magnetostriction data measured on fcc Co-Pd alloys, and using $\lambda_{111} = -\frac{1}{3} B_2^{\mathrm{fcc}} / c_{44}$.